Mathematical models and GNSS interference

GNSS Solutions:

Mathematical Models and GNSS Interference

"GNSS Solutions" is a regular column featuring questions and answers about technical aspects of GNSS. Readers are invited to send their questions to the columnists, **Professors Gérard Lachapelle** and **Mark Petovello**, Department of Geomatics Engineering, University of Calgary, who will find experts to answer them. Their e-mail addresses can be found with their biographies at the conclusion of the column.

What does "geometry-based" and "geometry-free" mean in the context of GNSS?

The geometry-based model is the usual mathematical model for solving high-precision positions from phase (and code) data using a relative GNSS receiver setup.

The relative receiver-satellite geometry plays a crucial role and has a significant effect on the precision of the parameters to be determined, which are, among others, the carrier phase ambiguities and the relative receiver position.

The geometry-free model dispenses this receiver-satellite geometry: it solves for the receiver-satellite ranges instead of positions. However, ambiguity resolution is still possible using this model.

To clarify this, recall the general observation equations for GNSS phase and code data:

$$\begin{aligned} \phi^s_{r,j} &= l^s_r + c\delta t_{r,j} - c\delta t^s_j + T^s_r - I^s_{r,j} + \lambda_j\left[\varphi_{r,j}(t_0) - \varphi^s_j(t_0) + N^s_{r,j}\right] + \varepsilon^s_{r,j} \\ p^s_{r,j} &= l^s_r + cdt_{r,j} - cdt^s_j + T^s_r + I^s_{r,j} + \in^s_{r,j} \end{aligned} \quad (1)$$

Here $\phi^s_{r,j}$ denotes the phase observable (in distance units) from satellite s to receiver r, tracked on frequency j and $p^s_{r,j}$ the corresponding code observable. The receiver-satellite range is denoted as l^s_r and the receiver clock errors for phase and code as $\delta t^s_{r,j}$ and $dt^s_{r,j}$, respectively. Satellite clock errors for phase and code are denoted as δt^s_j and dt^s, respectively, while T^s_r denotes the tropospheric and $I^s_{r,j}$ the ionospheric errors.

The initial phase of the signal at time of transmission is denoted as $\phi^s_j(t_0)$, and $\phi_{r,j}(t_0)$ denotes the initial phase of the signal generated in the receiver. The integer phase ambiguity is denoted as $N^s_{r,j}$ (in cycles), whereas the wavelength corresponding to frequency j is denoted as λ_j. In this context, we should mention that the term in square brackets is often referred to as *non-integer* (undifferenced) ambiguity.

Finally, all other remaining errors, such as multipath and receiver noise, are denoted as $\varepsilon^s_{r,j}$ for the phase observable and as $\in^s_{r,j}$ for the code observable.

The unknown receiver position is of course "hidden" in the receiver-satellite range:

$$l^s_r = \| x^s - x_r \| \quad (2)$$

where $x_r = (X_r, Y_r, Z_r)^T$ denotes the receiver coordinates and $x^s = (X^s, Y^s, Z^s)^T$ the satellite coordinates. To solve

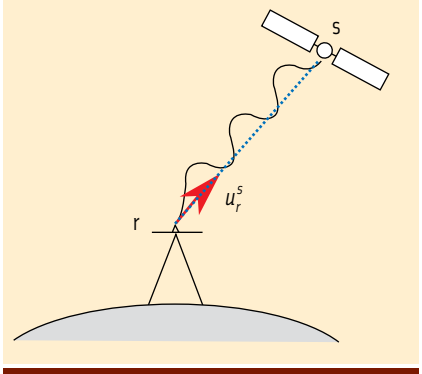

FIGURE 1 Unit direction or line of sight (LOS vector

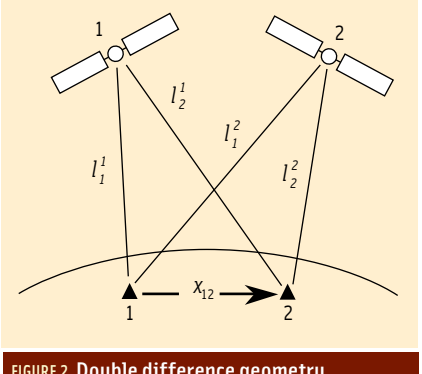

FIGURE 2 Double difference geometry

the receiver position, the phase and code observation equations need to be linearized as follows:

$$\Delta\phi^s_{r,j} = -(u^s_r)^T(\Delta x_r - \Delta x^s) + c\Delta\delta t_{r,j} - c\Delta\delta t^s_j + \Delta T^s_r - \Delta I^s_{r,j} + \lambda_j\left[\Delta\varphi_{r,j}(t_0) - \Delta\varphi^s_j(t_0) + \Delta N^s_{r,j}\right] + \varepsilon^s_{r,j} \quad (3)$$

$$\Delta p^s_{r,j} = -(u^s_r)^T(\Delta x_r - \Delta x^s) + c\Delta dt_{r,j} - c\Delta dt^s_j + \Delta T^s_r + \Delta I^s_{r,j} + \epsilon^s_{r,j}$$

where $u^s_r = (x^s - x^0_r)/||x^s - x^0_r||$ denotes the unit direction vector between receiver and satellite (line-of-sight vector), see **Figure 1**. Due to the linearization all observables and unknown parameters are denoted as incremental (delta) quantities.

In principle, for all these variables we need approximate values, which are denoted using the zero superscript. For example, in the linearization the receiver position is decomposed as $x_r = x^0_r + \Delta x_r$. It is assumed that the satellite positions are known (computed using either broadcast ephemeris or precise orbits), implying that $\Delta x^s = 0$.

To exploit the high precision of the phase data, the ambiguities need to be resolved to their integer values. This can be accomplished by a relative measurement setup in which GNSS data are simultaneously tracked by at least two receivers and two satellites in order to eliminate common errors. See **Figure 2**.

The resulting model of linearized observation equations is the *geometry-based model,* in which the position of the first receiver, the reference, should be known, and the relative position (baseline) of the second receiver is parameterized. This model is then usually based on double differences of the observables and parameters.

For example, the geometry-based model for a single epoch of dual-frequency phase and code data of m satellites tracked by two receivers reads, ignoring the differential ionospheric errors (this is allowed for short baselines):

$$\begin{pmatrix}\phi_1\\ \phi_2\\ p_1\\ p_2\end{pmatrix} = \begin{pmatrix}\lambda_1 I_{m-1} & 0\\ 0 & \lambda_2 I_{m-1}\\ 0 & 0\\ 0 & 0\end{pmatrix}\begin{pmatrix}a_1\\ a_2\end{pmatrix} + \begin{pmatrix}G\\ G\\ G\\ G\end{pmatrix} g + \begin{pmatrix}\varepsilon_1\\ \varepsilon_2\\ \epsilon_1\\ \epsilon_2\end{pmatrix} \quad (4)$$

with I_{m-1} the identity matrix of dimension m-1 and the following vectors defined as:

$$\phi_j = \begin{pmatrix} \Delta\phi^{12}_{12,j} \\ \vdots \\ \Delta\phi^{1m}_{12,j} \end{pmatrix} \quad p_j = \begin{pmatrix} \Delta p^{12}_{12,j} \\ \vdots \\ \Delta p^{1m}_{12,j} \end{pmatrix} \quad a_j = \begin{pmatrix} \Delta N^{12}_{12,j} \\ \vdots \\ \Delta N^{1m}_{12,j} \end{pmatrix} \quad g = \begin{pmatrix} \Delta X_{12} \\ \Delta Y_{12} \\ \Delta Z_{12} \\ \Delta T^{z}_{12} \end{pmatrix} \quad \varepsilon_j = \begin{pmatrix} \varepsilon^{12}_{12,j} \\ \vdots \\ \varepsilon^{1m}_{12,j} \end{pmatrix} \quad \in_j = \begin{pmatrix} \in^{12}_{12,j} \\ \vdots \\ \in^{1m}_{12,j} \end{pmatrix}$$

Thus the phase and code observables (plus their error components) are in double difference form, and the integer ambiguities as well. As a result of the double differencing all clock errors and initial phases are eliminated from the unknown parameter set; thus the ambiguities are now truly integer in nature.

As for the (differential) tropospheric errors, in the geometry-based model they are mapped to one delay in the local zenith, i.e.: $T^s_r = \Psi^s_r \, T^z_r$, where Ψ^s_r denotes the mapping coefficient. The mapping coefficients of all m satellites enter matrix G, together with the line-of-sight vectors, as follows:

$$G = \begin{pmatrix} -(u^2_2 - u^1_2)^T & (\psi^2_2 - \psi^1_2) \\ \\ -(u^m_2 - u^1_2)^T & (\psi^m_2 - \psi^1_2) \end{pmatrix} \quad 5$$

This matrix G is referred to as the (receiver-satellite) geometry matrix. We should point out that the geometry-based model is also solvable without the code data, but in that case at least two epochs of phase data should be included. At least five satellites are needed to solve the geometry-based model in which a tropospheric zenith delay is parameterized; in the absence of this parameter one needs at least four satellites.

Without linearization, the observation equations (1) themselves can still be used for ambiguity resolution. Instead of the receiver coordinates, one then solves for the receiver-satellite ranges. The resulting model is referred to as the *geometry-free model*.

For example, the geometry-free model for a single epoch of dual-frequency phase and code data of m satellites reads

$$\begin{pmatrix} \phi_1 \\ \phi_2 \\ p_1 \\ p_2 \end{pmatrix} = \begin{pmatrix} \lambda_1 I_{m-1} & 0 \\ 0 & \lambda_2 I_{m-1} \\ 0 & 0 \\ 0 & 0 \end{pmatrix} \begin{pmatrix} a_1 \\ a_2 \end{pmatrix} + \begin{pmatrix} I_{m-1} \\ I_{m-1} \\ I_{m-1} \\ I_{m-1} \end{pmatrix} \rho + \begin{pmatrix} \varepsilon_1 \\ \varepsilon_2 \\ \in_1 \\ \in_2 \end{pmatrix} \quad 6$$

where vector ρ represents the troposphere-biased receiver-satellite ranges, i.e. $\rho^s_r = l^s_r + T^s_r$.

Only these combined troposphere-range parameters are estimable, because the range and troposphere error cannot be distinguished from each other. This lumping can be seen as an advantage compared to the geometry-based model, because possible residual errors created by modeling the tropospheric delay do not affect ambiguity resolution.

Other differences exist between the geometry-free and geometry-based models. Because the geometry-free model is linear, in this model the original observations should be used, while in the geometry-based model these should be the "observed-minus-computed" observations. Because of this linearity, approximate values are not needed to solve the geometry-free model; also the model does not need a priori values for the satellite positions or the position of the reference receiver.

Another difference is that the geometry-free model can be solved using only two satellites, which means that the ambiguities corresponding to a single double difference can be resolved independently. Increasing the number of satellites does significantly benefit ambiguity resolution for the geometry-based model, but for the geometry-free model this improvement is only marginal.

One can easily demonstrate that the geometry-free model is weaker than its geometry-based counterpart, because in the latter model all ranges are coupled to the same three baseline components. Hence, the redundancy of the geometry-based model is higher and therefore its ability to detect outliers in the data is improved.

Finally we should mention that the geometry-free model cannot be solved without code data, because the absence of code data would make the design matrix, which consists of the columns of the two matrices in Equation (6), rank deficient.

In practice, the use of the geometry-free model is usually seen in combination with the geometry-based model for the purpose of ambiguity resolution. As a final remark one may argue whether the term "geometry-free" is completely justified here, as the receiver-satellite ranges are still present in the geometry-free model (a better name would be the "coordinate-free" model). In this context the well-known geometry-free *linear combination* of phase data is really geometry-free, because the receiver-satellite ranges are eliminated by taking the difference of the phase observables at two frequencies.

DENNIS ODIJK

Dr. Dennis Odijk is a researcher at Delft University of Technology. His interests are focused on, among others, GNSS ambiguity resolution and ionosphere modeling.

What are the main classes of interference that can degrade the GNSS signals? What are the possible countermeasures?

The extremely low received power of a GNSS signal makes it vulnerable to different kinds of interference, such as spurious and out-of-band emissions. These emissions can originate from telecommunication and electronic systems, either operating in adjacent bands or working at frequencies relatively far from the GNSS bands.

Interference can be intentional or unintentional. Intentional interference can be generated easily by GNSS jammers that adopt different strategies for jamming GNSS receivers, such as the emission of strong continuous waves (CW) or strong Gaussian noise occupying the same frequencies as the GNSS signal. Unintentional interference can be generated by a variety of sources, because every electronic device potentiallys emit strong electromagnetic signals that can jam the GNSS receiver.

Examples of unintentional interference are UHF and VHF television, VOR (VHF omnidirectional radio-range), and ILS (instrument landing system) harmonics and spurious signals caused by power amplifiers working in their non-linear region or by oscillators present in many electronic devices. Regardless of their source, interfering signals can generally be classified as *pulsed, continuous wave,* or *swept*.

Pulsed interference is characterized by intermittent bursts of signals, such as arise, for instance, from DME (distance measuring equipment) and the TACAN (TACtical Air Navigation) system. The former is a transponder-based radionavigation technology that measures distances by timing the propagation delay of VHF/UHF radio signals, whereas the latter is a navigation system used by military aircraft.

Both DMEs and TACAN emit series of pulse-pairs modulated at the frequencies in the range 962–1213 MHz. These frequencies include the Galileo E5 and GPS L5 bands; thus, DME/TACAN can represent a serious threat for GNSS receivers operating at these frequencies. The issue of DME/TACAN signals has been deeply analyzed in the literature and some details can be found in the article, "GNSS Album: Images and spectral signatures of the new GNSS signals," appearing in the June 2006 issue of *Inside GNSS*.

The class of continuous wave (CW) interference includes all those narrowband signals that can be reasonably

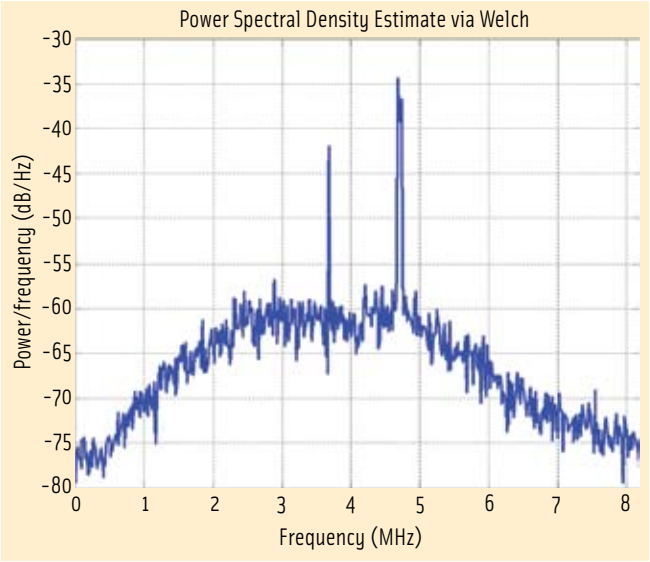

FIGURE 1 Power spectral density of a GPS signal corrupted by two CWs.

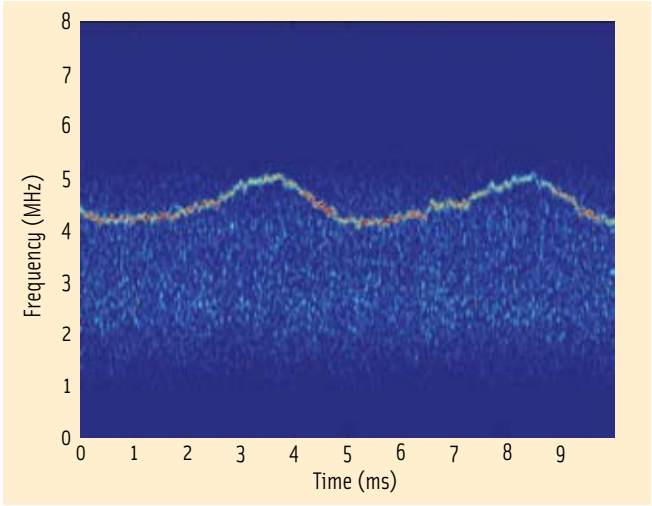

FIGURE 2 Spectrogram of a GPS signal corrupted by swept interference

represented as pure sinusoids with respect to the Galileo/GPS bands. Many electronic devices, such as personal computers and mobile phones, are equipped with local oscillators that can produce harmonics in the GNSS bands: these harmonics are examples of CW signals.

In **Figure 1** the power spectral density (PSD) of a GPS signal acquired by a GPS receiver front-end in the presence of a CW interferer is reported. As can be seen, the spectrum at the output of the front-end filter contains two peaks, each being a CW interference source.

Swept interferences are signals characterized by a narrow instantaneous band at a central frequency that changes over time. These interferences can be harmonics of frequency modulated (FM) signals and can be produced by telecommunication systems such as television and radio broadcasting.

An example of swept interference is depicted in **Figure 2**, which represents the spectrogram of a GPS signal acquired by means of a receiver front-end (thanks to L. Camoriano and T. C. G. Corsini for their support during data collection performed in Torino near the installation of different television emitters). The spectrogram represents the temporal evolution of the frequency content of the received signal:
— the faint, noisy band between 2 and 5 MHz represents the filtered and down-converted GPS signal the spectral characteristics of which are essentially stationary. The more prominent (red) line shows the sinusoidal evolution of the frequency content of the swept interference.

For each kind of interference, an appropriate countermeasure exists that exploits the time-frequency characteristics of the disturbing signal. One such method is based on spatial diversity, which effectively mitigates interference but is not discussed in detail here. Briefly, however, these techniques exploit the correlation between the received signals at different spatially separated antennas in order to minimize the interference impact. A short introduction to this topic can be found in "GNSS Solutions" of April 2006.

Aside from spatial diversity, interference mitigation techniques can be divided into time, frequency, and time-frequency algorithms according to the specific domain in which they operate.

Time domain mitigation techniques essentially consist of *excision* and *filtering*. Time excision is usually employed

for removing pulsed interference because pulsed signals are concentrated in the time domain. The few samples of the received GNSS signal that are affected by the interference are thus excised together with the interference without significantly affecting overall receiver performance.

Adaptive time filtering is generally used for removing CW and swept interference: an adaptive notch filter is, for instance, able to track the frequency variations of a swept signal and to efficiently mitigate its effects by placing a notch at the frequencies where the interference is most concentrated.

Adaptive filters are efficient devices requiring a low computational load and thus can be easily implemented in GNSS receivers; however, their use is often limited to mono-component signals. Special solutions have to be adopted if more than one CW or swept signal is present.

In frequency domain mitigation algorithms, the GNSS signal is FFT (fast Fourier transform)-transformed, processed, and inverse FFT-transformed back into the time domain. The FFT allows the CW and pulsed interference to be concentrated in the frequency domain, where they can be easily excised. These techniques can effectively handle multi-component signals and thus can cope with more than one interfering signal.

A drawback of frequency domain algorithms appears in the fact that a swept interference source, when FFT transformed, can occupy a large portion of the digital frequency range. This makes efficient excision more difficult, because the quality of the GNSS signal can be seriously compromised if too many frequency bins are removed.

A solution can be found in time-frequency mitigation techniques: the received signal is first expanded into the time-frequency plane by means of an appropriate time-frequency transformation such as the spectrogram. In this domain the interference is well localized, as in Figure 2, and thus can be removed with a little degradation of the GNSS signal. Once the interference is excised, the time domain signal is reconstructed.

Mark Petovello is an assistant professor in the Department of Geomatics Engineering at the University of Calgary. He has been actively involved in many aspects of positioning and navigation since 1997 including GNSS algorithm development, inertial navigation, sensor integration, and software development.

Email: mpetovello@geomatics.ucalgary.ca

Professor Gérard Lachapelle holds a CRC/iCORE Chair in Wireless Location in the Department of Geomatics Engineering at the University of Calgary. He has been involved with GNSS since 1980 and has received numerous awards for his contributions in the area of differential kinematic GPS and indoor location.

Email: lachapel@geomatics.ucalgary.ca

The use of time-frequency mitigation techniques is limited by the high computational load required to transform the signal into the time-frequency plane. However, as the technology continuously evolves, such techniques may be adopted in future GNSS receivers. Because they are able to cope with a large variety of interfering signals, they combine the advantages of both time and frequency mitigation algorithms.

Manufacturers

The data in figures 1 and 2 was derived from a NordNav-R30 receiver from **NordNav** (now a part of **CSR,** Cambridge, England).

DANIELE BORIO AND LETIZIA LO PRESTI

Daniele Borio (daniele.borio@polito.it) is a Ph.D student at the Politecnico di Torino in Turin, Italy. His research activity is mainly focused on GNSS signal acquisition. **Letizia Lo Presti** (letizia.lopresti@polito.it) is full professor at the Politecnico di Torino. Her fields of expertise include digital signal processing, communications, and navigation. IG